Energy Science & Engineering

Open Access

RESEARCH ARTICLE

Photovoltaic monitoring system for Auger Muons and Infill for the Ground Array

Angel Cancio Montbrun[1,2], Alexis Mancilla[1], Javier Maya[1], Beatriz García[1,3], Alejandro Almela[2,4], Belén Andrada[4,5], Ana M. Botti[4,6], Alberto Etchegoyen[2,4], Juan M. Figueira[4,5], Alan Fuster[2,4], Nicolas González[4,6], Matías R. Hampel[2,4], Ewa Holt[4,6], Johannes Hulsman[4,6], Mariela Jose Bachuili[4,5,6], Nicolas Leal[1], Agustín Lucero[2,4], Diego Melo[4], Sarah Müller[4,6], Matías Perlin[4], Manuel Platino[4], Diego Ravignani[4], Matias Roncoroni[4], Federico Sánchez[4], Christian Sarmiento-Cano[4], David Schmidt[4,6], Gaia Silli[4,6], Federico Suarez[2,4], Alvaro Taboada[4,6], Oscar Wainberg[2,4], Brian Wundheiler[4,5] & Diana Yelós[1]

[1]Instituto de Tecnologías en Detección y Astropartículas (CNEA, CONICET, UNSAM), Regional Cuyo, Comisión Nacional de Energía Atómica, Mendoza M5501CIG, Argentina
[2]Facultad Regional Buenos Aires, Universidad Tecnológica Nacional, CABA C1179AAQ, Argentina
[3]Facultad Regional Mendoza, Universidad Tecnológica Nacional, Mendoza M5502AJE, Argentina
[4]Instituto de Tecnologías en Detección y Astropartículas (CNEA, CONICET, UNSAM), Centro Atómico Constituyentes, Comisión Nacional de Energía Atómica, Buenos Aires B1650KNA, Argentina
[5]Departamento de Física, Facultad de Ciencias Exactas y Naturales, Universidad de Buenos Aires, Buenos Aires, Argentina
[6]Institut für Kernphysik (IKP), Karlsruhe Institute of Technology, Karlsruhe 76021, Germany

Keywords
AMIGA Project, monitoring, photovoltaic System

Correspondence
Angel Cancio Montbrun, Instituto de Tecnologías en Detección y Astropartículas (CNEA, CONICET, UNSAM), Regional Cuyo, Comisión Nacional de Energía Atómica, Mendoza M5501CIG, Argentina. E-mail: angel.cancio@iteda.cnea.gov.ar

Funding Information
Ministerio de Ciencia Tecnología e Innovación Productiva, Comisión Nacional de Energía Atómica, Gobierno de Argentina, Consejo Nacional de Investigaciones Científicas y Técnicas.

Received: 25 February 2018; Revised: 11 April 2018; Accepted: 3 May 2018

Energy Science and Engineering **2018; 6(4): 289–305**

doi: 10.1002/ese3.197

Abstract

This study is devoted to characterizing the operation of the entire photovoltaic system installed in one of the Auger Muons and Infill for the Ground Array (AMIGA) stations, a complimentary detector for the Pierre Auger Observatory, the largest cosmic-ray air shower array in the world, 3000 km^2, powered exclusively by solar energy. To understand charge and discharge cycles, the whole system behavior under different climatic conditions and to determine its limitations, the design of a new prototype for monitoring the whole system online is a fundamental part of this contribution. Also, it is demonstrated that the configuration of solar charge controllers in parallel is able to manage panels of different powers and brands and that the monitoring system allows analyzing periods with adverse weather conditions.

Introduction

The stand-alone photovoltaic system (PVS) studied in this contribution is an enhancement of the PVS implemented at the Pierre Auger Observatory [1, 2] for the Auger Muons and Infill for the Ground Array project (AMIGA) [3–6]. The Pierre Auger Observatory is the largest cosmic-ray air shower array detector in the world, with 1660 surface detectors (SD) distributed in 3000 km^2 and 27 fluorescence telescopes installed in four buildings located

at the edge of the array, devoted to the studies of ultra high-energy cosmic rays which arrive from outer space to the upper layers of the atmosphere and produce particle air showers that reach the surface of the Earth. On the other hand, AMIGA project was designed to have a direct measurement of the muonic component of these showers and constitutes an improvement between the scientific facilities in Malargüe, Mendoza.

The Observatory works thanks to a unique photovoltaic macro-grid constituted by 1660 identical stand-alone PVS. The first studies about the system to provide energy to the array were made by López Agüera and Rodríguez Cabo [7] before completing the installation of the Observatory and where the authors also proposed the study of weather variables on the PVS behavior. After more than 10 years taking data each 10-min continuously, is possible to have a good statistics about the performance of solar panels, batteries, and the whole system installed in Marlargüe, devoted not only to assure correct functioning of the SD, since the failures in the SD array system means data losses, but also to design new installations and to obtain a better response and a more confident control of performance. With these data were possible to propose a method for the estimation of the state of the lead-acid batteries, based on the evolution of voltage distribution along the time of use [8]. In this frame of work, we can assure that the Observatory worked without critical fails during this long time baseline, but new instruments and detectors imply more energy consumption. This is the case of AMIGA, which will require 61 stations powered by an own stand-alone PVS that includes solar panels, solar charge controllers and a battery bank (with AGM Super Cycle batteries) for energy storage in order to supply power during the night or low solar radiation conditions, in the same way as the SD but with a highest power requirement: the power consumption of each module, including its own communication system and auxiliary electronics was measured, at the laboratory, and results of 46.3 W, as is shown in Table 1 [9]. In this sense, it is important to assure autonomy taking into account eventual bad weather conditions and local weather conditions in general, one of the main proposals in this paper. For this reason, a monitoring system for this new stand-alone PVS is also part of the present development.

It is known that different weather conditions change the efficiency of the PVS [10], we do not study in detail the solar panels in their structure, but we will take as part of this study the performance under different weather conditions with the aim to know if the proposed system will meet the muon detector array power requirements, determining accurate current–voltage and power–voltage relationships which define the number of panels and batteries for the system.

Table 1. An estimated power consumption of Auger Muons and Infill for the Ground Array electronics installed in the unitary cell at the selected surface detector "Los Piojos".

Component	Size (m^2)	Consumption (W)
Module A	10	9.7
Module B	5	9.7
Module C	5	9.7
Module D	10	9.7
Auxiliary electronics		3.5
Comms		4.0
Total	30	46.3

AMIGA is a facility designed to reach two stages: (1) the Unitary Cell (UC), that consists of seven SD stations on an hexagonal grid equipped with muon scintillators (MC), located near Coihueco FD building (see Fig. 1) with the purpose of debugging the engineering issues and understanding the counting uncertainties in order to reach the final design for the production array, this is a prototype of the main AMIGA array, and (2) the production array of AMIGA which will consist of 61 stations of muon counters detectors.

Each AMIGA station consists of a standard Auger SD station (see Fig. 2) and three or four scintillator modules achieving a total detection area of 30 m^2.

The design proposed for the AMIGA PVS [9] was focused on the final stage (production) of AMIGA array and it was based on experiences and knowledge gained during the prototype stage (UC). As the electronics of the detector is also part of the development and changed along the process which defined the final product, the photovoltaic was designed using the measurements made in the laboratory, without the knowledge of the consumption and performance of the station in the field. For this, it was necessary to monitor and evaluate the PVS under real conditions. The proposed PVS, was installed at "Los Piojos" station (Lat.:−35.11°; Long: −69.55°) (Fig. 1); it has two solar panels (220 and 170 Wp) installed with a tilt angle of 45° and North orientation, each one connected to its own solar charge controller. The solar panels are mounted on a pole at 1.50 m height. This height is similar to the distance measured from the ground to the base of the solar panel of the SD station. The location of the solar panel was determined by the soil condition and the positions of the modules in each site. The solar charge controllers are connected in a parallel configuration to the battery bank. Furthermore, the AMIGA station is powered through one of the two solar charge controllers (see Fig. 3).

There are a several data acquisition systems (DAQs) to evaluate the PV plants, which is a fundamental task to improve this kind of resources [11]. Nevertheless,

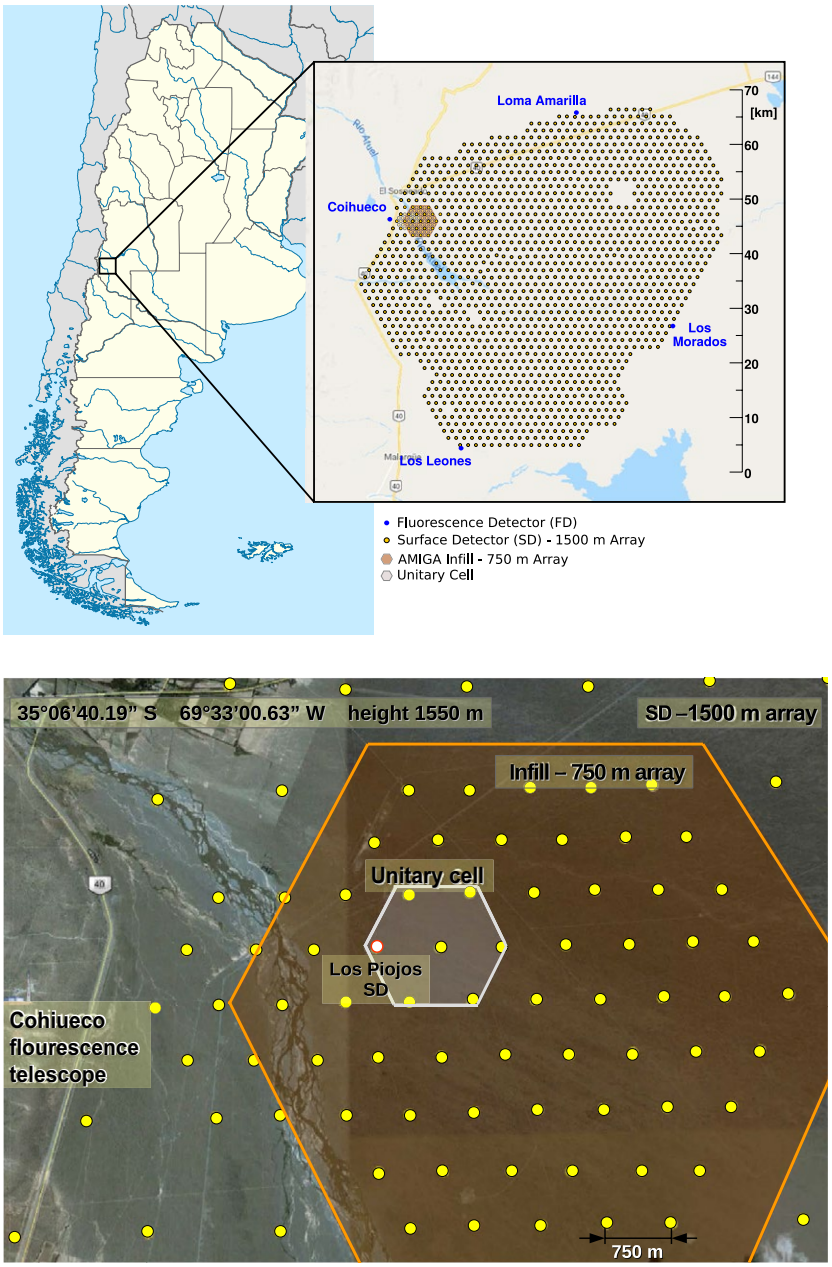

Figure 1. Pierre Auger Observatory has 1660 surface detectors (SD) distributed in 3000 km^2 that constitute a 1500 m array grid and 27 fluorescence telescopes installed in four buildings located at the edge of the array. The Infill array has 61 detectors at 750 m one each other. The Unitary Cell and the SD "Los Piojos'' are inside of the Infill, where the monitoring device for the photovoltaic system of AMIGA is installed. AMIGA, Auger Muons and Infill for the Ground Array.

in this paper we decide not only to make a complete new experimental study of the performance of the proposed AMIGA PV systems on site but also monitoring that system with a new user-centered DAQ in order to decide on the variables, the results accessibility, the graphical representations and to (a) determine the real power consumption that must be provided to each AMIGA station, (b) understand the behavior of the whole system (AMIGA PVS and AMIGA detector), (c) calculate the autonomy of the entire system, and (d) have the experimental results which will allow to characterize the PVS and redesign or correct the photovoltaic setup, if it is needed, (e) permit an online monitoring of the system, taking into account that the

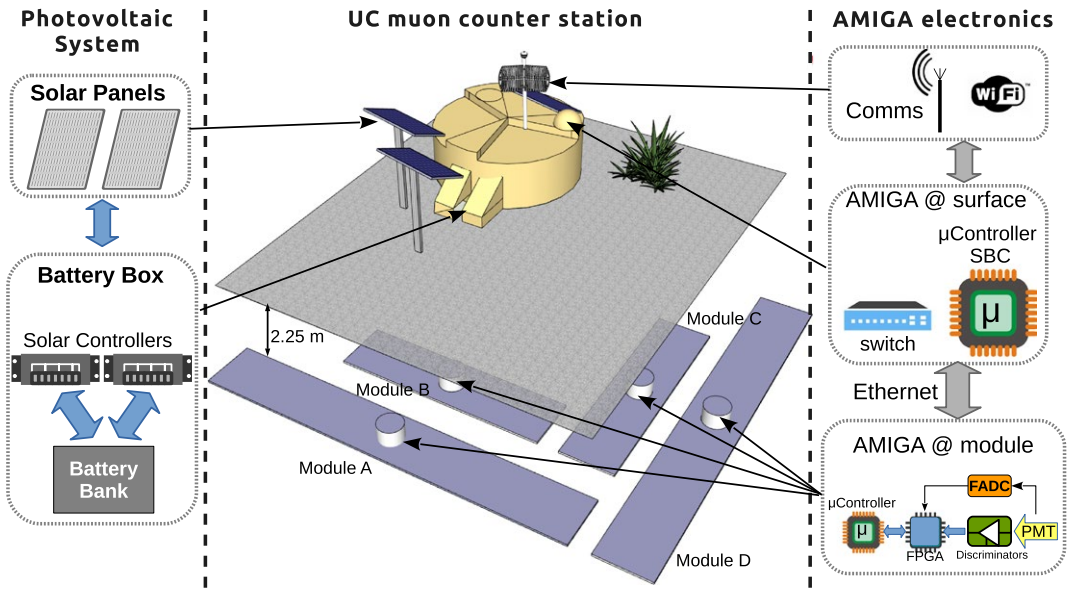

Figure 2. AMIGA station [3] is accompanied by a 30 m^2 scintillator counter buried at a depth of 2.3 m to shield from the electromagnetic particles and directly count muons, it has three or four modules underground, auxiliary electronics, comms, and a photovoltaic stand-alone system that includes solar panels, solar charge controllers, and a battery bank. AMIGA, Auger Muons and Infill for the Ground Array.

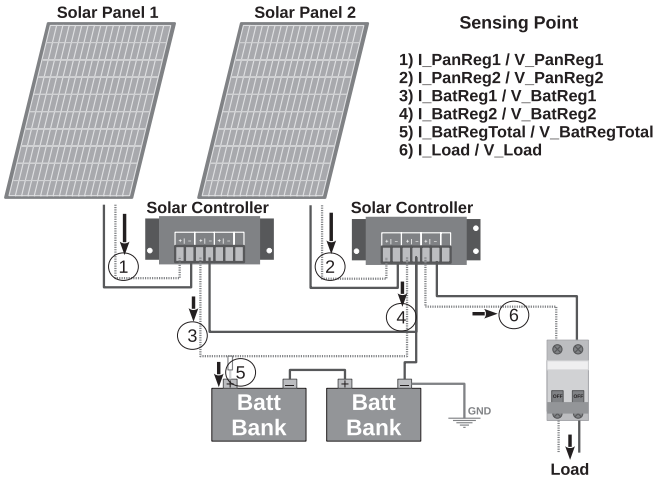

Figure 3. AMIGA photovoltaic system with two solar panels, a battery bank, and two solar charge controllers with the battery output connected in parallel to the battery bank. Also, it shows the disposition of sensors for measure voltages and currents. AMIGA, Auger Muons and Infill for the Ground Array.

Pierre Auger Collaboration is distributed on almost all the Globe.

In the following sections we discuss the PVS design (Section "System design"), the design and characteristics of the monitoring system (Section "Measurement method of the PVS"), the general performance (Section "Performance and results") and the AMIGA electronics real power consumption, after a year of collecting measurements in the field (Section "PVS power calculation").

System Design

As we mentioned in a previous section, the AMIGA PVS (see Fig. 3) consists of two solar panels (220 Wp Pevafersa® and 170 Wp Atersa®, see Table 2), a battery bank (two 165 Ah batteries AGM Super Cycle batteries Victron® Energy, see Table 3), and two solar charge controllers (Morningstar SUNSAVER®, model SS-10L-24V 3rd generation, see Table 4) with the battery output connected in parallel to

Table 2. Solar panel specification parameters. Current at short circuit (Isc), Voltage at open circuit (Voc), Max. voltage (Vpm) at maximum power (P_{max}), Max. current (Ipm) at P_{max}, Alpha (α): Temperature coefficient of solar panel Isc., Beta (β): Temperature coefficient of solar panel Voc. and Gamma (γ): Temperature coefficient of solar panel P_{max}, and nominal operating cell temperature (NOCT).

	Pevafersa IP-VAP-220	Atersa A-170P
P_{max} (W±3%)	220	170
Number cells	60	72
Imp (A)	7.68	4.72
Vmp (V)	29.30	36.05
Isc (A)	8.20	5.0
Voc (V)	37.31	44.25
α Isc (%/°C)	0.0317	0.08
β Voc (%/°C)	−0.331	−0.32
γ P_{max} (%/°C)	−0.505	−0.38
Max voltage (V)	1000	1000
NOCT (°C)	47 (1±1%)	47 (1±2%)
Dimensions (mm)	1641×989×46	1618×817×35

Table 3. Deep cycle AGM battery specification parameters.

	Victron Energy BAT412151084
Watt-hour at C20 (Wh)	1980
Amp-hour at C20 (Ah)	165
Voltage (V)	12
Dimensions (mm)	485×172×240
Weight (kg)	47
Cold cranking Amps (CCA) at 0°F	1200
Reserve capacity at 80°F	320
General specification	
Technology: flat plate AGM	
Terminals: copper	
Rated capacity: 20 h discharge at 25°C	
Float design life: 7–10 years at 20°C	
Cycle design life	
400 cycles at 80% discharge	
600 cycles at 50% discharge	
1500 cycles at 30% discharge	

the battery bank [12–15]. Because manual measurements are insufficient to fully determine how the entire system works, it was decided to install a continuous monitoring device of voltages and currents, in order to characterize the whole system to optimize its performance. To describe how the charging system behaves, we must know how the solar charge controllers work, because they are responsible for managing the energy taken by the panels and for providing this energy to the load and to the battery bank.

The Morningstar solar charge controller [15] chosen for the project has an algorithm of four stages (see Fig. 4) to quickly, efficiently, and safely charge the battery bank:

Table 4. Solar controller specification parameters

	Morningstar SS-10L-24
System voltage (V)	24
Min. battery voltage (V)	1
Regulation voltage	24
Sealed battery	28.2
Flooded battery	28.8
Load voltage disconnect (V)	23.0
LVD reconnect (V)	25.2
Max. solar voltage (V)	60
Load in-rush capability (A)	65
Voltage accuracy (mV)	±48
Battery charging	
Temperature compensation coefficient (mV/°C)	−60
Range (°C)	−30 to +60

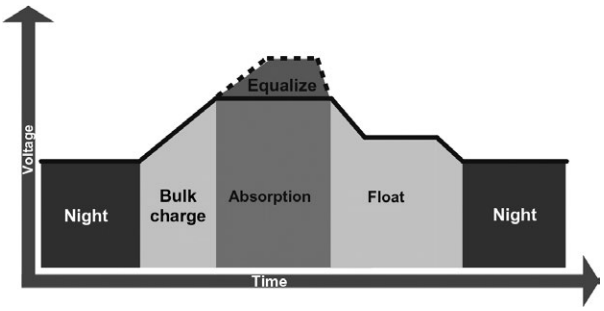

Figure 4. SunSaver charging algorithm, four stages battery sequency charge [15].

- Bulk Charge: In this stage, the battery voltage has not reached absorption voltage yet, and 100% of available solar power is used to recharge the battery.
- Absorption: When the battery has been recharged to the absorption voltage set-point, constant-voltage regulation is used to prevent heating and excessive battery gassing.
- Float: After the battery is fully charged the SunSaver reduces the battery voltage to a float charge which is sometimes called a trickle charge. Depending on battery history, the battery remains at the absorption stage for 3 or 4 h before transitioning to the float stage.
- Equalization: The SunSaver equalizes a flooded battery for 3 h every 28 days. This process prevents the stratification of the electrolyte and equalizes the voltages of the individual elements within the battery.

The PVS does not use flooded batteries, so the equalization function is off in the solar charge controller and for its characterization it is necessary to place voltage and current sensors at different points in the system, at the same places where the measurements were manually performed before. This allows identifying how the batteries are charged by

Table 5. Simplified current flows analysis of the Auger Muons and Infill for the Ground Array station photovoltaic system at each sensor.

	Current						
Status	I_1	I_2	I_3	I_4	I_5	I_6	Observations
Battery bank discharged and sunlight	+	+	+	+	+	+	Panel 1 is charging the battery bank while Panel 2 supply current to the Load and the remaining power is supplied to the battery bank.
Battery bank charged and sunlight	+	0	+	–	0	+	Panel 1 supply current to the Load and Panel 2 is at Open Circuit. Without considering the maintenance charge stage made by the solar controller.
Battery bank discharging and night	0	0	–	–	–	+	Battery Bank supply current to all system, to both solar controllers and to the load.

panels, and how solar charge controllers manage this power to the load. The operation expected by the manufacturer of the regulator can be checked, too. The measurements are stored in a data logger.

Simplified description of the currents flow

As it is shown in Figure 3, the arrows represent the positive direction of the currents flows used for this analysis. Also, the current consumption of the solar controllers (Ireg1 and Ireg2) is <8 mA, which is considered negligible for this description. Now we can express the currents as follows:

1. $I_1 = I_{\text{panel1}}$
2. $I_2 = I_{\text{panel2}}$
3. $I_3 = I_{\text{panel1}} - I_{\text{reg1}}$ where $I_{\text{reg1}} < 8$ mA $\rightarrow I_3 \approx I_{\text{panel1}}$
4. $I_4 = I_{\text{panel2}} - I_6 - I_{\text{reg2}}$ where $I_{\text{reg2}} < 8$ mA $\rightarrow I_4 \approx I_{\text{panel2}} - I_6$
5. $I_5 = I_3 + I_4$
6. $I_6 = I_{\text{Load}}$ where I_{Load} is the consumption of interest

Width this equations we can express the current flows description for three possible scenarios (see Table 5): (1) Battery Bank Discharged and Sunlight, (2) Battery Bank Charged and Sunlight, and (3) Battery Bank Discharging and Night. Of course there is the case of Battery Bank Discharged and Night but in this case the system is off.

Measurement Method of the PVS

Data logger prototype

A "data logger prototype" [16] was proposed and installed in the AMIGA PVS, located at "Los Piojos" SD station, for testing of the device. In this location, the AMIGA detector has four modules, the auxiliary electronics, and the communication system. However, a new prototype which enhances connectivity and remote access since it incorporates a Single Board Computer (SBC) for network connection and a Peripheral Interface Controller (PIC) to improve the robustness of the system, was build and installed for this study. It uses, as a power source, the AMIGA battery bank.

This prototype consists of three parts: (1) Sensing, based on six ACS712 [17] current sensors and six resistive dividers for voltage measurement; (2) Acquisition, based on a PIC18F4520 microcontroller with 12 ADC to take the data from the sensors; (3) Storage and communications, based on a TS-7260 SBC, responsible for receiving data from the PIC 18F4520, storing and sending it to the server for processing.

Sensing

Current sensors

The ACS712 is a Hall effect sensor. It has three possible formats, to measure up to 5 A, 20 A, and 30 A. The difference between each of the models is the response curve slope of the output voltage based on the sensed current, thus for any model its analog output varies between 0 and 5 V giving better resolution to the model which measures up to 5 A than the one that measures up to 30 A, according to the manufacturer.

For the PVS, it is necessary to measure currents that can reach up to 7.68 A in the 220 Wp solar panel, 15 A in the battery bank terminal during the charging stage and up to 2 A in the AMIGA detector. For this, we decided to use sensors of ±20 A for measuring high currents in panels and batteries, and sensors of ±5 A for measuring the current of AMIGA electronics.

It should be noted that these sensors have an error of ±1.5% at full measurement scale.

Sampling at a higher frequency is needed to perform a postprocessing that involves making statistical operations in order to minimize this error.

Voltage sensor

We use a resistive voltage divider because the measured voltages vary between 0 and 45 V. This reduces the voltage to adjust the value to the input of the ADC since it only allows voltages from 0 to 5 V.

Temperature and humidity sensor

The possibility of using a temperature and humidity sensor (SHT71) on the batteries was considered because the solar charge controller has a correction coefficient that makes a variation in voltage changes at the regulation stages. This is important because the battery voltage can reach up to 30 V with decreasing temperature in winter, but this will be implemented for a new version of the data logger. Although, the batteries, the solar controllers, and the monitoring system are installed inside of a battery box, which is designed to keep the temperature and humidity relatively stable. It should not affect the measurements or results of this work. The Pierre Auger Observatory does not measure the temperature and surface humidity of the panels, therefore, for the comparison of results, it was not taken into account either.

Acquisition

Microcontroller

The outputs of the six current sensors and six voltage dividers were connected to the ADC inputs of the PIC18F4520 microcontroller, programmed to receive commands through a serial port (set to 9600 bps 8N1) and store the measured data as comma separated values.

Single board computer

To record the acquired data by the electronics and in order to transfer the log files, we used a TS7260 SBC, which has a low power consumption (≈1 W). The SBC manages the data from the microcontroller through a serial port, using a shell script that save this data as comma separated values every minute. The script puts a time-stamp (in UNIX time) at the beginning of each data array obtained from the microcontroller and save the register every day in one file called "YYYMMDD.CSV". The files are stored in a directory in the SBC, where each row contains a register.

Storage and communication

Data files are generated by acquiring 160 kB per day and are stored locally in the SBC. The data transfer is performed using a local Internet connection through a restricted access to the SBC, allowing direct transmission of data to external servers (at the laboratory) for further analysis.

Software design

The software to manage the data at the data logger was implemented to recover and save the measured voltage and current values at each sensing point (voltage and current for the batteries, regulators and the whole system) in comma separated (CSV) files and encoded by the microcontroller when they are acquired and recorded for simplicity [18].

The acquired data are processed by a script developed in Python language, which imports the records acquired each day, creating a table inside a MySQL database. The fields of this table correspond to the sensors and data logger and the index corresponds to the time-stamps of each record time UTC Unix Epoch (Local Time = UTC - 3 h). The general idea is to learn from this development in order to design a monitoring system integrated to the AMIGA electronics in the near future.

The encoded values registered in the CSV files are converted to the corresponding actual value of voltage (V) and current (I) before being stored in the database, according to the particular reference value of the data logger, using the expressions

$$V = \left(\frac{\text{Measured value} \times \text{reference}}{1023} \right) \times 11 + V_{\text{offset}} \quad (1)$$

$$I = \left(\frac{\text{Measured value} \times \text{reference}}{1023} - 2.5 \right) \times \frac{1}{C_1} + C_{\text{offset}} \quad (2)$$

where C_1 is a coefficient that depends on the sensor used at the sensing point. V_{offset} and C_{offset} are calibration values.

The intrinsic error of the sensors is ±1.5%, but the measured error of the whole system is between 4 and 10%, as is observed in 1 and 2, where the constant threshold values were obtained by contrasting the monitoring system with a patron device and manual measures. So, the adjustment is for the entire circuit of the monitoring electronics and not for the particular sensors. We must clarify that there is a detriment in the accuracy when we measure values that vary from 0 to 5 A and values that vary from 0 to 15 A, all with the same sensor, so the resolution is less accurate to measure mA, but it was decided to use the same type of sensor for all measurement points in

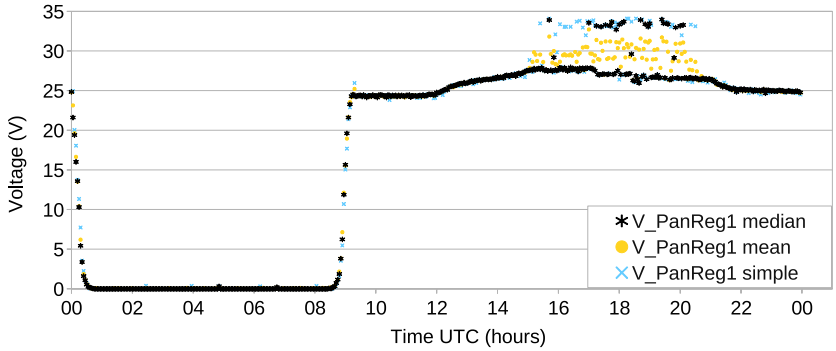

Figure 5. Panel voltage data smoothing using different filters, the median filters shows the best response during all day, especially during the night where the solar panel current must be zero.

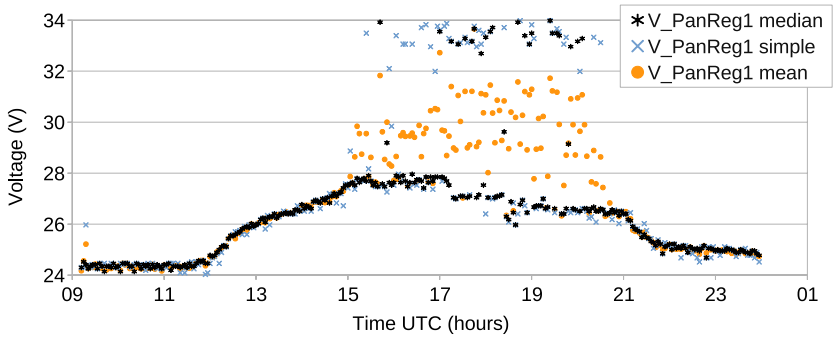

Figure 6. Panel voltage data smoothing using different filters and its behavior during sunlight, during the float stage the voltage switches between two values and only the median and simple filter has a good response.

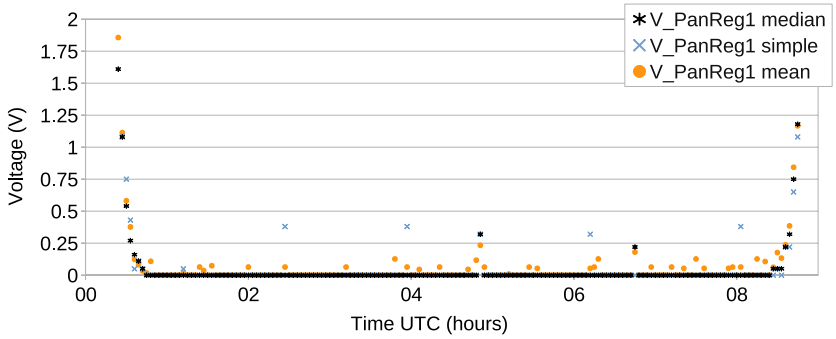

Figure 7. Panel voltage data smoothing using different filters and its behavior during night, it can be seen that the median filter is the more accurate and gives zero voltage for the solar panel output.

order to standardize future maintenance. And using a smooth filter in postprocessing we mitigate this error.

The script running on the server is also used to plot time series and to upload those graphics to an FTP server. In this way, the information is available for downloading and visualization. The records are exported in XLSX or CSV format for later integration with another system, like the monitoring systems of Pierre Auger Observatory.

After conducting a continuous analysis of the acquired data, it was found that the instrument error can be reduced through a data postprocessing. There are many ways of smoothing the time-series data: the simple filter which chooses one sample every 3 min, the mean filter which takes the average of 3 min of sampled data, and the median filter which consist in selecting the closest value to the median of the selected dataset, this results in one sample per chosen period, in this case 3 min data. Figure 5 shows the effect of three filters.

For a better visualization, Figures 6 and 7 show the behavior of each filter during sunlight and night,

respectively. The mean filter cannot handle the data that change abruptly between two values inside the temporal window (this effect is caused inside of the solar charge controller due to the behavior of the Pulse Width Modulation, or PWM), and the resulting values are wrong. It can be seen that the mean filter and the simple filter have more noise than the median filter, during the night where the panel voltage must be zero, both filters show positive values. The classical median filter restricts the output value to be the same as the value of one of the samples in the observation window [19] and although the median filter offers little flexibility and is temporal blind, all temporal information is lost in the filtering process, we can still use the median filter because all samples have the same weight.

Summarizing, the only filter that is more accurate during the entire day is the median filter because it does not select a random value, it selects the central value of an ordered subset of data. That is why we can use it to smooth the error or noise of the measurements. We can see this in Figure 7 during the night where the panel voltage must be zero.

So the postprocessing consists of increasing the sampling frequency rate in order to perform a downsampling at a lower frequency by applying a median filter to the dataset, this results in one sample per chosen period (i.e., sample rate of 1 sample every 10 sec, and downsampling to 1 sample every 180 sec). This method is used to reduce the intrinsic instrument errors (sensor error) and the dataset is smoothed by removing data that deviate from typical values. The algorithm steps are: (1) create an array with contiguous samples from the data, (2) sort the array in order (from min to max), (3) find the median value of the array, if dataset is even, choose one of the two middlemost numbers, (4) add the selected value to a new array, with the time-stamp that correspond to the first sample in this window, and (5) start from (1) with the next set of samples, repeat until the end.

Calibration

To verify the data measured by the data logger, a comparison was made with manual measurements obtained with commercial equipment (Fluke 179 and UNI-T UT200 Series). The calibration was performed with the error analysis, where two correction parameters, a current offset of 340 mA and a voltage offset of 250 mV were determined. These offsets are added by the software during the uploading to the database.

Data visualization

The processed data are plotted daily and posted on a website for visualization. A data-sheet file corresponding to the data each day, is published on the website and available for download. The website is updated every 10 min. Using the same script defined before, the time series plots, for a required number of days, can be generated from the command line, as well as the graphics of stacked data by day and hour.

Performance and Results

Morningstar stages algorithm

With the measurements and analysis made on the voltage data of the terminals of the solar charge controller (Reg1), it was found that the results are in agreement with the manufacturer data-sheet, as is shown in Figure 4. The four stages of the charging algorithm, measured directly from the battery terminal of the solar charge controller (Reg1) of the PVS, are presented in Figure 8. The controller sets a voltage of 28.2 V [15] to start the absorption stage and 3 h to complete it; this stage is after the bulk charge stage. A voltage of 27.4 V is needed for the flotation stage. These data were corroborated by the data logger, evaluating the voltage of the solar charge controller (Reg1).

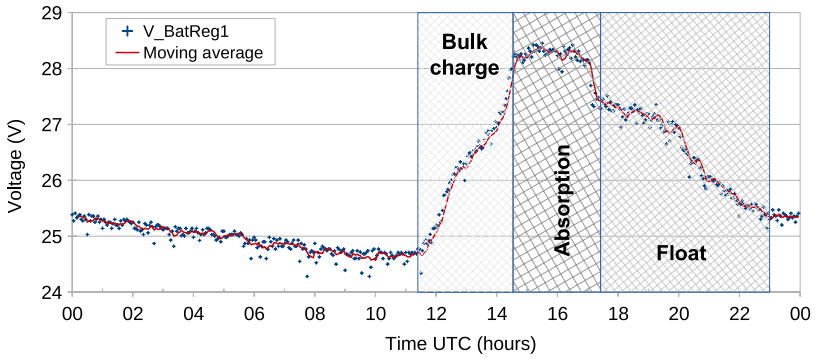

Figure 8. Moving average of PVS: battery bank voltage at solar charge controller (Reg1). We can identify the four stages of the charging algorithm, measured directly from the battery terminal of the solar charge controller. PVS, photovoltaic system.

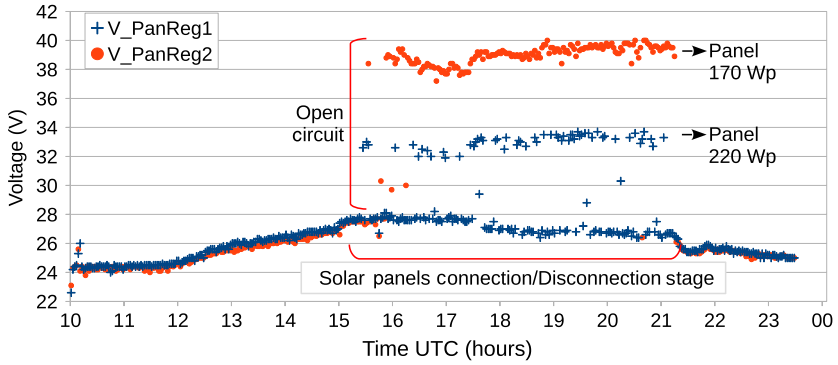

Figure 9. Voltage for panel Reg1 and panel Reg2, the solar charge controller begins a stage of connection and disconnection showing the open circuit voltage of each panel after the bulk charge stage.

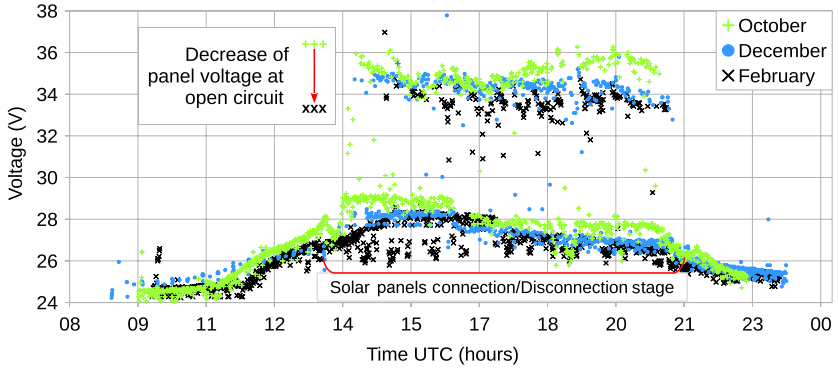

Figure 10. Voltage for panel Reg1 for the 15th of every month between October 2015 and February 2016. We can see the voltage of one of the panels in the open circuit stage, decreased from October to February, this is due to the tilt angle used in the panels.

Panel-controller connection

Each panel is connected to a solar charge controller. The moment when the solar charge controller begins a stage of connection and disconnection can be identified, showing the open circuit voltage of each panel, after the bulk charge stage (Fig. 9 shows the panel voltage during a day). With this voltage, we could identify the panel that is connected to each solar charge controller, because we know that the 170 Wp panel has higher open circuit voltage than the 220 Wp one [20]. You can also see which solar panel is connected to the load and which is kept disconnected during this stage.

In Figure 10 we detect that the voltage of one of the panels in the open circuit case decreased from October to February. This is because the tilt angle used in the panels is fixed to improve the efficiency in winter. During the year, sun rays strike the panels in a different angle, being closer to perpendicular during spring and autumn.

Evaluation of cut-off by low battery voltage

Figure 11 shows a cut-off produced by the solar charge controller due to low voltage in the battery on October 11, 2015. After a week with adverse weather conditions, the battery did not reach the minimum operating voltage of 23 V, which is the cut-off voltage by under voltage, preset by the manufacturer in the solar charge controllers. As shown in the Figure 11, the controller reconnects the charge at 25 V. The cut-off voltage and the re-connection voltage allows checking the correct operation of the solar charge controller and also check in the data logger status.

On the other hand, Figure 11 also shows that the cut-off occurs at the end of the night (11:00 UTC) after sunrise the solar charge controller takes approximately 5 h to reconnect the load safely for the weather conditions of this day.

The previous analysis reveals that it is necessary to modify the wiring of the photovoltaic system in order to increase up time, even in adverse climate weeks.

Modification of photovoltaic wiring system

After analyzing the conditions in which the solar charge controller cuts off the power supply, it is possible to conclude that it is necessary to connect the load to the

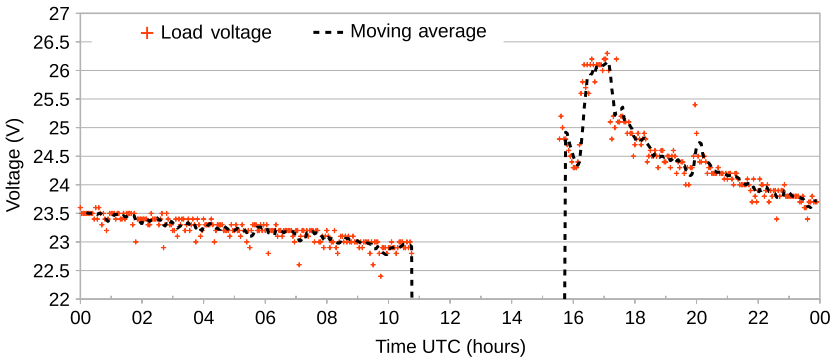

Figure 11. Load voltage cut-off and re-connection, the solar controller cut-off the load voltage at 23 V and reconnect when the voltage reaches 25.2 V.

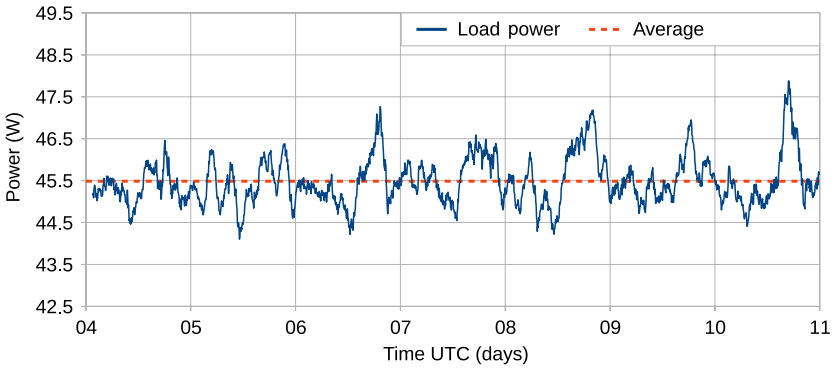

Figure 12. Load power (consumption) from January 1 to 11, 2016. The load power integrated average corresponds to 45.5 W.

terminal of the battery to ensure that the solar charge controller will not cut off due to low battery voltage. This could reduce the lifetime of the battery. To solve this issue, it is advisable to place a protective low voltage circuit with a voltage less than the cut-off of the solar charge controller. According to the manufacturer, we get into critical voltage conditions when the battery is at 10.8 V. In order to protect the batteries, it would be possible to set the critical voltage value to 11 V, which for a 24 V battery bank will be 22 V and still keep a safety factor.

Average load power

Evaluating data in the data logger from January 1 to 11, 2016, it was found that the consumption of the load is around 45.5 W for an AMIGA detector with four modules, one auxiliary electronics, and communication (Fig. 12). This results correspond to an average of 25 V and 1.82 A.

Power delivered by the panels to the systems

The daily power of individual panels from January 4 to 10, 2016 can be seen in Figure 13. It is evident how cloudy days (January 5 and 9, 2016) affect the power delivery to the system. The power fall and return to the initial value, we can infer that this effect is due to the passage of a cloud, particularly on January 5th we can identify three spikes, although this type of system analysis should be confirmed with direct images, a task which will be considered as future work.

Referring to the panels, it should be clear that the real power that can be extracted is at battery voltage rather than maximum output voltage of the panels; for example, for the 220 Wp panel, the current at the point of maximum power (I_{mp}) is 7.68 A, so, the maximum power at 25 V will be 192 W. This value is important because it allows clarifying, that with a 24 V battery bank, it is stored less power than the nominal power of the panels. This can be verified by looking at the plots of the power panels for different weather conditions.

PVS Power Calculation

With the data from the monitoring device it is possible to calculate the installed capacity of the photovoltaic system at Los Piojos station. To make this calculation, the voltage and current delivered by the battery when the panels are

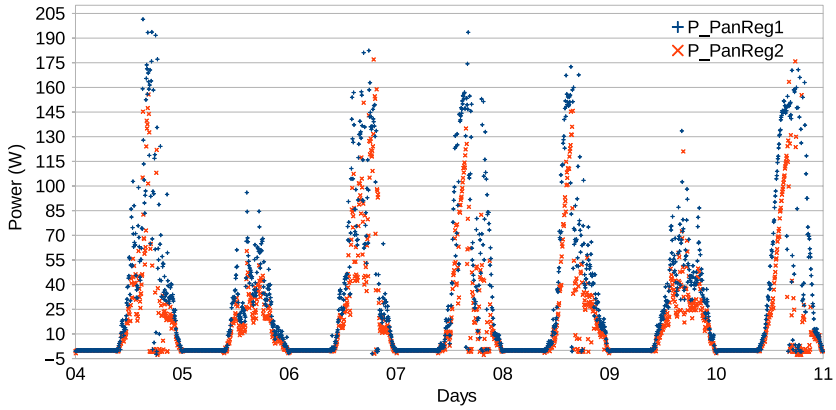

Figure 13. Power of solar panels from January 4 to 10, 2016. We can identify two days, 5 and 9, with clouds that affect the power delivery to the system.

not delivering power, must be considered. The data from the monitoring system to be used are the total current from the batteries (I_Bat_T) and the battery voltage at the solar charge controller 2 (V_Bat_Reg2). For the final estimation, the elements of the photovoltaic system and the location will be used. The average load power, voltage, and current were estimated in subsection "Average load power".

Energy supplied by the panels

If we define the "Peak Sun-Hours" (or HPS) as the time (measured in units of hours) per day that we have a hypothetical constant solar irradiance of 1000 W/m^2 per unit time, then one peak solar time "HPS" is equivalent to 1000 Wh/m^2, or 3.6 MJ/m^2 per hour. It is a way of accounting the energy received from the Sun grouping them into packages, and each "package" of 1 h receives 1000 W/m^2 (the relation to the SI unit is thus 1 kW/m^2 = 24 kWh/m^2/day).

The PVS has two solar panels of 220 and 170 Wp. In the present case, the daily energy of each panel will be calculated separately and then added together to obtain the total daily energy delivered. The expression that will be used is [21]:

$$E_p = W_{mp} \times \mathrm{HPS} \times \eta_p \quad (3)$$

where W_{mp} corresponds to the peak power or maximum power of the panel, HPS is the factor related to the hours per day of maximum solar irradiation on the surface, and η_p corresponds to the panel performance with typical values between 85 and 95%. As standard, it is possible to choose a general performance of 95%, and for this, the conversion factor is 0.95.

The solar irradiation in the surface depends on the position (geographical coordinates) where the photovoltaic system is located. In this case, the reference is the position of the Malargüe airport. AMIGA site, is approximately 45 km north of Malargüe Airport. The distance between this two places is not significant and it is taken as valid for the irradiation measure obtained at Malargüe Airport; this value is used to calculate the performance of the PVS.

The irradiation value used for the calculation was taken from the worst condition of sunlight for a year (June), at Los Piojos position. The global solar irradiation data for Malargüe Airport were calculated using the RETScreen 4 software,[1] using the data based on the observations of more than 200 satellites, which provide meteorology and solar energy parameters, monthly averaged from 22 years of data for a particular location (latitude and longitude),[2] sponsored by NASA's applied Science Program, at the Atmospheric Science Data Center.

Monthly averaged parameters from the period of July 11, 1983 to June 30, 2005 and daily averaged solar and meteorological data over the time period July 1983 to June 2005 are available. The solar energy data are generated using the Pinker/Laszlo shortwave algorithm [22]. Cloud data are taken from the International Satellite Cloud Climatology Project DX dataset (ISCCP).[3]

In general, the irradiation values are measured on the horizontal surface of the chosen site, RETScreen-4 software can correct the irradiation values for any angle of the solar panel. For the current design, the solar panels are installed at 45°. Finally, daily values of irradiation for the period 2005 to 2015 measured on the surface (at 0°) and also corrected for the 45° inclination, were included. These data are monthly averaged for each year from 2005 to 2015, and finally averaged for 10 years (see Tables 6 and 7).

The irradiation value for calculations of energy from solar panels was selected taking into account the worst

Table 6. Monthly global irradiation on the surface at Malargüe Airport, ICAO Code: SAMM (kWh/m^2/day).

Site	Jan	Feb	Mar	Apr	May	Jun	Jul	Aug	Sep	Oct	Nov	Dec
SAMM	8.04	6.96	5.94	4.4	2.91	2.24	2.47	3.05	4.61	6.05	7.48	8.04

Table 7. Monthly global irradiation at Malargüe Airport, ICAO Code: SAMM (kWh/m^2/day) using a correction for 45°.

Site	Jan	Feb	Mar	Apr	May	Jun	Jul	Aug	Sep	Oct	Nov	Dec
SAMM	6.6	6.42	6.53	5.9	4.68	3.92	4.13	4.23	5.31	5.86	6.34	6.4

solar conditions for the studied site, which occurs in June when the "maximum altitude" of the sun above the horizon is the lower (35°), and the daylight number of hours is the minimum (10 h). Considering that (1) the irradiance is the magnitude describing radiation intensity or solar lighting reaching us as a measure of instantaneous power per unit area (W/m^2 or equivalent units), the irradiance value measured under standard conditions is 1000 W/m^2, and (2) the irradiation is the amount of irradiance received in a given period of time, that is, the power received per area unit integrated in time (which is typically measured in Wh/m^2 or equivalent units), in order to calculate the HPS value, we divide the value of the incident irradiation by the value of the power of irradiance under standard conditions, because these conditions are met when the electrical characteristics of photovoltaic modules are also met [21]. Table 7 shows the irradiation obtained at the evaluated location. The result for June is 3920 Wh/m^2 per day, which is the lower value that corresponds to winter at southern hemisphere.

The value of the daily energy supplied by the panel of 220 Wp (E_{p220w}) [20], considering that the HPS is 3.92 hours per day, can be calculated using 3,

$$E_{p220w} = (220\,W_p \times 3.92\,h \times 0.95) = 819.28\,Wh. \quad (4)$$

On the other hand, the same quantity supplied by the panel of 170 Wp (E_{p170w}) [20], is,

$$E_{p170w} = (170\,W_p \times 3.92\,h \times 0.95) = 633.08\,Wh. \quad (5)$$

Then, the total daily energy supplied is,

$$E_p = E_{p220w} + E_{p170w} = 819.28\,Wh + 633.08\,Wh = 1452.36\,Wh. \quad (6)$$

If the panel performance, η_p, is changed to the lower typical value of 85%, the total energy supplied will be:

$$E_{p220w} = (220\,W_p \times 3.92\,h \times 0.85) = 733.04\,Wh. \quad (7)$$

$$E_{p170w} = (170\,W_p \times 3.92\,h \times 0.85) = 566.44\,Wh. \quad (8)$$

$$E_p = E_{p220w} + E_{p170w} = 733.04\,Wh + 566.44\,Wh = 1299.48\,Wh. \quad (9)$$

AMIGA detector energy consumption

The energy consumed by the load is calculated using the photovoltaic monitoring system database, from which, the average current consumption is 1.82 A and the battery voltage is 25 V; the average power consumption of load is 45.5 W.

$$E_c = 45.5\,W \times 24\,h = 1092\,Wh. \quad (10)$$

Then, the daily total energy consumption by the load is 1092 Wh per day (E_c), which is lower than the daily total energy supplied by the solar panels, E_p. In consequence, the solar panels supply enough energy to operate the AMIGA station.

Theoretical value of PVS autonomy

Autonomy of the photovoltaic system is understood as the number of days with little or no solar irradiation in which the electronics must work, that is, the facility needs to operate without being supplied with energy from the panels. The required battery energy to assure autonomy [21], can be estimated by,

$$E_b = \frac{(E_{max} \times N_d)}{P_d} \quad (11)$$

where E_b is the battery energy (Wh), E_{max} is the energy needed for the load to work for 1 day (Wh), N_d is the number of autonomy days that must work the load, and P_d is the depth of battery discharge (usually takes the value 0.6 dimensionless) [21, 23].

As the battery bank is already installed, it is possible to obtain, from equation 11, the number of days of system autonomy, N_d. The load energy consumption includes the energy consumption of the associated electronics, the four modules, the communications and the energy consumption of the PVS components, as well as the energy losses by the PVS (Table 8). Using the calculated value of 1092 Wh for the energy consumed by the load in a day, the number of autonomy days with the actual setup is:

Table 8. Numbers of days of autonomy of the photovoltaic system for different consumption values with the same battery bank.

$E_{consum(load)}$ (Wh)	$E_{consum(loadperday)}$ (Wh) at 25 Volt	$E_{battery}$ (Wh)	Days of autonomy
30	720	3960	3.30
35	840	3960	2.83
40	960	3960	2.48
45.5	1092	3960	2.17
47	1128	3960	2.11
50	1200	3960	1.98
55	1320	3960	1.80

$$N_d = \frac{P_d \times E_b}{E_{max}} = \frac{0.6 \times 3960\,\text{Wh}}{1092\,\text{Wh}} = 2.17\,\text{days}. \quad (12)$$

Real value of PVS autonomy

In order to determine the autonomy time of the AMIGA PVS, we must evaluate its behavior under adverse climatic conditions to obtain data of battery discharge, and disconnection of the load. These conditions are given when there is low intensity of sunlight. In order to carry out the analysis, the days between July 1 and 5, 2016 were selected, because this time period starts with a favorable climatic day in which the batteries are charged, followed by two overcast days whit rain in which the batteries are discharged and not fully recharged during the day, and end with 2 days of favorable weather conditions in which the batteries recover their charge.

The batteries of the analyzed PVS have been working for several months, and the PVS has undergone cycles of cut-off and recovery due to unfavorable climatic conditions, which leads us to have a system with real operation conditions and allows us to perform a correct analysis. If the batteries had been new and with maximum charge, the analysis would had been biased. In Figure 14 we show four stacked charts for each day selected for analysis. Plot (14A) presents the rainfall data for the Coihueco site (≈4 km to the AMIGA PVS), plot (14B) shows the currents of each solar panel, plot (14C) show the voltages of each panel, and plot (14D) shows the voltage at the load. At day 1 the solar charge controller goes into a state of maintenance of load which means that the batteries were fully charged and we can infer that it was a sunny day. On days 2 and 3 the battery charge cycle was not complete, the current did not reach the normal peak value (≈ 11 A) which is the sum of the current of the two panels (see Fig. 14B), the voltage of the panels remain constant (≈ 24 V) (see Fig. 14C) and we can infer that the weather conditions were unfavorable, cloudy and/or rainy as shown in Figure 14A. Due to unfavorable weather conditions extending for 2 days, on day 3 at 10:45 h UTC the solar charge controller disconnect the load voltage (at ≈ 23 V, Fig. 14D). During this cut-off the battery charge gets recovered, but the load voltage remains cut-off until it reaches ≈ 25 V, due to the solar charge controller behavior. In the night of day 3, occurs the second cut-off. At day 4, a complete normal charge cycle of the batteries takes place, which means that the weather conditions improved. Again, the load voltage remains cut off until it reaches ≈ 25 V. Day 5 shows a normal operating cycle of the power system.

The variation in the load voltage during the discharge of the batteries in unfavorable weather conditions (days 1, 2, and 3 of the previous analysis) can be evaluated from Figure 15. It can be observed that at approximately 23 V the solar charge controller cuts off the power supply to the load, in order to avoid a deep discharge of the batteries. The discharge time until reaching the cut-off voltage is 39 h, which represents a real autonomy of 1.6 days that is less than the 2.17 days obtained from the theoretical calculation. This difference between theoretical autonomy and real autonomy can be the product of the drop in the performance of the panels, the performance of the batteries, and the climatic conditions of the days before the power cut-off.

Figure 15 also shows the trend line of voltage drop that is directly related to the discharge of the batteries, taking into account its slope and extrapolating we can estimate the time needed to reach 21.6 V, meaning that each battery reaches the limit determined by the manufacturer, 10.8 V. Regarding this limit the battery undergoes a deep discharge without endangering its useful life.

The recommendation to extend the autonomy range while maintaining the 45.5 W consumption of the electronics is to connect the load directly to the terminal of the battery bank and place an external system to shut off the power supply when the voltage reaches approximately 22 V and reset the connection at 25 V, leaving a safety margin.

PVS power lost

When working, the photovoltaic system has its own energy consumption. This "lost" energy is composed of: (1) the one used by solar charge controllers, (2) the one lost by auto-discharge of the battery, (3) the one lost by performance of the batteries, and (4) the one unpredictably lost (Joule effect, down of tension, etc.) [21]. The power in the load (W_{max}) is built by the electronics power consumption (W_{elec}), plus the power lost by the photovoltaic system itself (W_L), and results,

$$W_{max} = W_{elec} + W_L. \quad (13)$$

The energy in the load and the consumed power of the electronics are obtained from the PVS monitoring database. The average value for W_{elec} is 44.82 W. From this, it is possible to obtain the PVS power lost (W_L), which results in 0.18 W.

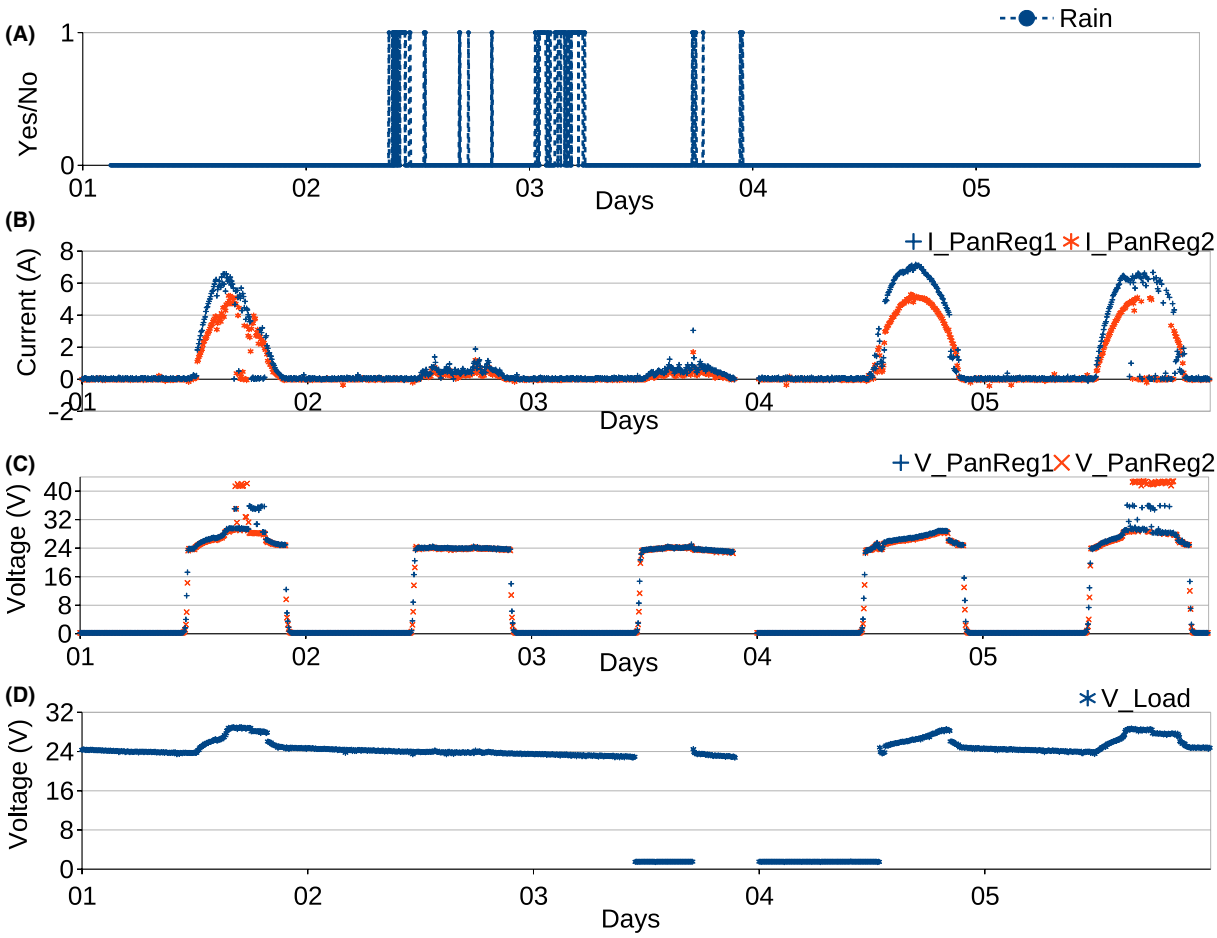

Figure 14. Top to bottom: (A) Rainfall at Coihueco, (B) solar panel 1 and 2 current, (C) solar panel 1 and 2 voltage, and (D) load voltage.

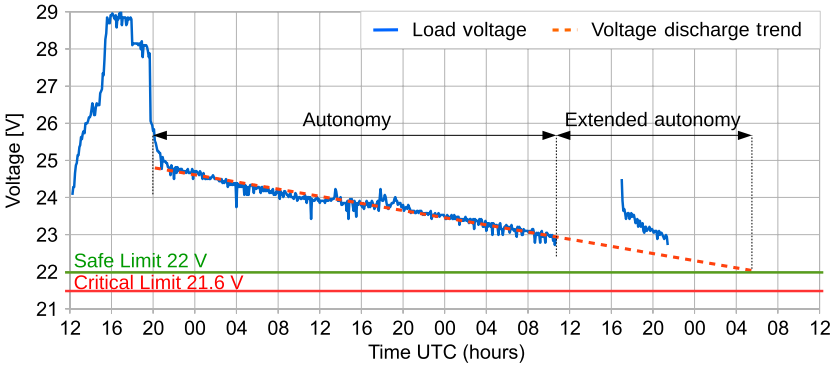

Figure 15. Autonomy measures by evaluation of load voltage during battery discharge.

The integration of the monitoring system to the AMIGA electronics could be evaluated, to reduce the number of components, to maintain the control on the PVS and in order to assure the solution of eventual problems mainly during the bad weather condition periods.

Conclusions

From the work presented in this paper, it was possible to characterize the operation of the entire AMIGA PVS. The analysis of charge–discharge cycle and the behavior under different climatic conditions were used to know limitations

of the system such as days of autonomy, times of charge/discharge, currents peaks, and voltages, which are fundamental results to propose a production design.

It was determined that the configuration of solar charge controllers in parallel is able to manage panels from different powers and brands. The monitoring system allows analyzing periods with adverse weather conditions by indirect detection of clouds.

The global power consumption of AMIGA station installed at Los Piojos is ≈ 45.5 W, which is near to the 46.3 W measured in the laboratory (for four muons counters). The current configuration allows 2.17 days of autonomy in theory for a consumption of 45.5 W. The analysis of a year of data reveals a real autonomy of 1.6 days. To increase the autonomy, it is necessary to modify the existing wiring, directly connecting the load to the battery bank terminal and implementing a low voltage cut-off protection with a lower limit than that provided by the solar charge controllers, without modifying the others photovoltaic system components. With this change, the system has an additional operating time and can avoid cutting the power to the load, avoiding the loss of data.

To improve the actual knowledge of the AMIGA PVS based on the experience gained, the development of a new data logger must includes:

- The use of voltage and current sensors with better resolution.
- The addition of temperature and humidity sensors at the battery box.
- Data preprocessing during the measuring, to reduce the noise.

In the case of the change in the photo-detector (e.g., from PMTs to SiPMs) as is part of the actual proposal for the muon detector [24], the consumption of the new electronics will change and the PVS can be re designed, now with a complete knowledge of the critical variables.

Finally, the use of local renewable energy resources is of fundamental importance to meet the actual demands of energy. The PVS appears as one of the most accessible possibilities because the costs, easy installation, and maintenance, but the climatic factor as temperature, wind speed, and solar radiation are important variables at the time to define their performance [25]. This study contributes to understanding part of this conditions in a special site in the world where, eventually and because the weather conditions, one Photovoltaic Energy Plant could be installed.

Acknowledgments

The authors thank the MINCyT and CONICET and the permanent support of Pierre Auger Observatory staff. The careful revision of the article by Rubén Piacentini is also very much appreciated, his suggestions improved significantly the article.

Conflict of Interest

None declared.

Notes

[1] RETScreen 4 software http://www.nrcan.gc.ca/energy/software-tools/7465

[2] Data available from the "Surface meteorology and Solar Energy, a renewable energy resource website" see http://power.larc.nasa.gov/ and https://eosweb.larc.nasa.gov/cgi-bin/sse/sse.cgi?skip@larc.nasa.gov

[3] ISCCP: http://isccp.giss.nasa.gov/

References

1. Aab, A., P. Abreu, M. Aglietta, E. Ahn, I. Al Samarai, I. Albuquerque et al. 1996. The Pierre Auger project design report. Tech. Rep. FERMILAB-PUB-96-024, FERMILAB-DESIGN-1996-02, FERMILAB, Batavia, IL.
2. Aab, A., P. Abreu, M. Aglietta, E. Ahn, I. Al Samarai, I. Albuquerque et al. 2015. The Pierre Auger cosmic ray observatory. NIMA, 798.
3. Aab, A., P. Abreu, M. Aglietta, E. Ahn, I. Al Samarai, I. Albuquerque et al. 2016. Prototype muon detectors for the AMIGA component of the Pierre Auger Observatory. JINST 11:P02012.
4. Etchegoyen, A. 2007. AMIGA, auger muons and infill for the ground array. In Proceedings, 30th International Cosmic Ray Conference (ICRC 2007): Merida, Yucatan, Mexico, July 3–11, 2007, vol. 5, 1191–1194.
5. Etchegoyen, A., U. Fröhlich, A. Lucero, I. Sidelnik, and B. Wundheiler. 2010. The Pierre Auger project and enhancements. AIP Conference Proceedings, 1265, 129–138.
6. Suarez, F. 2013. The AMIGA muon detectors of the Pierre Auger Observatory: overview and status. In Proceedings, 33rd International Cosmic Ray Conference (ICRC2013): Rio de Janeiro, Brazil, July 2-9, 2013, 0712. Available at http://www.cbpf.br/%7Eicrc2013/papers/icrc2013-0712.pdf.
7. Agüera, A. L., and I. R. Cabo. 2007. The Pierre Auger Project as a challenging tool for studying PV systems. Renew. Energy Power Qual. J. 2011;10:1005–1010.
8. Agüera, A. L., I. R. Cabo, and D. R. Rey. 2011. Algorithm for lifetime estimation of batteries based on voltage distribution shape. Environ. Eng. Manag. J. https://doi.org/10.24084/repqj05.290.
9. Videla, M., A. Almela, A. Cancio, A. Fuster, F. Gallo, M. Hampel et al. 2015. Photovoltaic system design for the AMIGA project. Tech. rep., Pierre Auger Observatory. GAP2015_058, priv. comm.

10. Van Dyk, E. E., A. R. Gxasheka, and E. L. Meyer. 2005. Monitoring current-voltage characteristics and energy output of silicon photovoltaic modules. Renewable Energy 30:399–411.
11. Rezk, H., I. Tyukhov, M. Al-Dhaifallah, and A. Tikhonov. 2017. Performance of data acquisition system for monitoring PV system parameters. Measurement 104:204–211.
12. Maya, J., A. Mancilla, M. Videla, and B. García. 2015a. Assembly of Atersa 170wp solar panel bracket. Tech. rep., ITeDA. IT-AM-41, priv. comm.
13. Maya, J., A. Mancilla, M. Videla, and B. García. 2015b. Installation of the photovoltaic system for the unitary cell of AMIGA. Tech. rep., ITeDA. Procedure IT-AM-39, priv. comm.
14. Maya, J., A. Mancilla, M. Videla, and B. García. 2015c. Installation of the photovoltaic system for the unitary cell of AMIGA, Anexx. Tech. rep., ITeDA. Procedure IT-AM-39ANNEX, priv. comm.
15. Morningstar Coorporation. 2011. "SunSaver PV System Controllers" installation and operation manuals. Data Sheet. Available at http://www.morningstarcorp.com/wp-content/uploads/2014/02/SS3.IOM_Operators_Manual.01.EN_pdf.
16. Cancio, A., A. Mancilla, J. Maya, N. Leal, M. Youinou, A. Almela et al. 2016. Photovoltaic monitoring system for AMIGA. Tech. rep., Pierre Auger Observatory. GAP2016_024, priv. comm.
17. Allegro MicroSystems. 2007. Sensor ACS712. Data Sheet. Available at https://www.sparkfun.com/datasheets/BreakoutBoards/0712.pdf.
18. Cancio, A., A. Mancilla, J. Maya, N. Leal, A. Almela, B. Andrada et al. 2017. Monitoring software: AMIGA photovoltaic system. Tech. rep., Pierre Auger Observatory. GAP2017_011, priv. comm.
19. Arce, G. R., Y. Kim, and K. E. Barner. 1998. 20 Order-statistic filtering and smoothing of time-series: Part I. Pp. 525–554 Order statistics: applications, vol. 17 of Handbook of statistics. Elsevier, Amsterdam, the Netherlands.
20. Atersa. 2008. Módulo Fotovoltáico A-170P, 2008, ref MU-5P 6x12-K. Data Sheet. Available at http://www.atersa.com/img/MU-5P_6x12-K_A170180P.Pdf
21. Aparicio, M. 2010. Energía solar fotovoltáica. Marcombo, ediciones marcombo edn.
22. Pinker, R. T., and I. Laszlo. 1992. Modeling surface solar irradiance for satellite applications on a global scale. J. Appl. Meteorol. 31:194–211.
23. Victron Energy B.V. (2016) Baterías gel y AGM, data sheet. Available at https://www.victronenergy.com.es/upload/documents/Datasheet-GEL-and-AGM-Batteries-ES.pdf edn.
24. Aab, A., P. Abreu, M. Aglietta, E. Ahn, I. A. Samarai, I. Albuquerque et al. 2017. Muon counting using silicon photomultipliers in the AMIGA detector of the Pierre Auger Observatory. JINST 12:P03002.
25. Zhou, W., H. Yang, and Z. Fang. 2007. A novel model for photovoltaic array performance prediction. Appl. Energy 84:1187–1198.

